IRON, COPPER AND TIN INCORPORATED RICE HUSK ASH SILICA: PREPARATION, CHARACTERIZATION AND APPLICATION AS CATALYSTS FOR FRIEDEL-CRAFTS BENZOYLATION REACTIONS

ISHRAGA ABDELMONIEM HASSAN

UNIVERSITI SAINS MALAYSIA

2011

IRON, COPPER AND TIN INCORPORATED RICE HUSK ASH SILICA: PREPARATION, CHARACTERIZATION AND APPLICATION AS CATALYSTS FOR FRIEDEL-CRAFTS BENZOYLATION REACTIONS

By

ISHRAGA ABDELMONIEM HASSAN

Thesis submitted in fulfillment of the requirements for the degree of
Doctor of Philosophy

UNIVERSITI SAINS MALAYSIA

July 2011

ACKNOWLEDGMENTS

In the name of Allah, the most Gracious, the most Merciful

I would like to take this opportunity to express my sincere feeling of gratitude to my supervisor Prof. Farook Adam for his patience, encouragement, continuous support, unlimited guidance and fruitful advice throughout this research.

I am pleased to extend my thanks and gratitude to the government of Sudan, the government of Malaysia, University of Khartoum, Universiti Sains Malaysia and School of Chemical Sciences for their financial, academic and technical supports. I would also like to thank the Malaysian Government and Universiti Sains Malaysia for the research grants under E-Science Fund grant (Ac. No.: 305/PKIMIA/613317) and Research University grant (Ac. No.: 1001/PKIMIA/814019), which were used to support this work.

I wish to express my special appreciation to Dr. Radhika for giving me worthy advice, valuable suggestions and constructive discussions.

My personal thanks also extended to the technical staffs: Mr. Kanthasamy, Mr. Aw Yong, Mr. Yee, Mr. Ong Chin Hwie, Mr. Rosli, Madam Saripah, Mr. Karuna, Mr. Muthu, Mr. Jauhar, Mrs. Faiza and Madam Jamilah for their kind help in the nitrogen sorption analysis, XRD, CHN, AAS, GC-MS and electronic microscope analysis. I would like to thank Ibnu Sina Centre (UTM, Malaysia), Combicat centre (UM, Malaysia) and IIT institute (India) for their help in running the solid-state NMR and EPR analysis.

Many friends as well as coworkers have helped me during my research. In particular, I would like to thank Dr. Adil Elhag Ahmed for his special assistance. I would like to thank my friends Mrs. Abeer, Dr. Elham, Mr. Anwar Iqbal, Ms. Jeyashelly, Mr. Kassim, Ms. Hanani and my uncle Dr. Abdel Raheem. I would like

to acknowledge the staff members of Faculty of Science, University of Khartoum, specially, Dr. Bushra, Dr. Hassan Nimr, Dr. Osman, Dr. Mohammed, Mrs. Islah and Mrs. Nuha Fathi, who had encouraged me to pursue higher studies.

I am always deeply obliged to my parents (Abdelmoniem Hassan and Gamalat Sayed), my brothers Mohamed, Ahmed and Kamal, and my sister Iynas for their continuous encouragement and support towards my higher degree in science. I will never forget their spiritual support, continuous praying and doaa to Allah for help. My acknowledgements are also to my father, mother, brothers and sisters in law for their encouragement and spiritual support.

Last but not least, I wish to express my warm and sincere appreciation to my husband Dr. Naser Eltaher and my lovely son Abdelmoniem for their patience, support and continuous encouragement in achieving my ambition**.**

TABLE OF CONTENTS

		Page
Acknowledgement		ii
Table of contents		iv
List of tables		x
List of figures		xii
List of schemes		xv
List of abbreviations		xvi
List of symbols		xviii
List of appendices		xix
Abstrak		xxiii
Abstract		xxv
Chapter 1 – Introduction		
1.1	General introduction	1
1.2	Rice husk (RH)	3
1.2.1	Properties and chemical composition of rice husk	3
1.2.2	Rice husk ash (RHA)	4
1.2.3	Preparation and purity of silica from RHA	5
1.2.4	Application of the silica extracted from RHA	7
1.2.5	Applications of the silica as adsorbents and catalyst support	8
1.3	Catalysis and catalyst	9
1.3.1	Classification of catalysts	10

1.3.2 Supported catalysts 12

1.4 Friedel-Crafts reactions 13

1.4.1 Friedel-Crafts acylation 14

1.4.2 The difference between Friedel-Crafts type acylation and alkylation reactions 15

1.4.3 Homogeneously catalyzed acylation 15

1.4.4 Heterogeneously catalyzed acylation 17

1.4.5 Green chemistry and solid acids 19

1.5 Scope of the thesis 20

1.6 Research objectives 21

Chapter 2- Experimental

2.1 Raw material and chemicals 23

2.2 Catalysts preparation 23

2.2.1 Treatment of rice husk 23

2.2.2 Extraction of silica as sodium silicate 24

2.2.3 Preparation of silica 24

2.2.4 Preparation of iron-rice husk silica 25

2.2.5 Preparation of copper-rice husk silica 25

2.2.6 Preparation of tin- rice husk silica 26

2.3 Physico-chemical characterization of catalysts 26

2.3.1 Powder X-ray diffraction (XRD) analysis 27

2.3.2 Fourier transform-infrared analysis (FT-IR) 27

2.3.3 Nitrogen adsorption-desorption measurment 27

2.3.4 Determination of metal content by atomic absorption spectroscopy (AAS) 28
2.3.5 Scanning electron microscopy (SEM) analysis 28
2.3.6 Energy dispersive X-ray (EDX) analysis 29
2.3.7 Transmission electron microscopy (TEM) analysis 29
2.3.8 Diffuse reflectance UV-Vis analysis (DR UV-Vis) 29
2.3.9 Solid state ^{29}Si MAS nuclear magnetic resonance (^{29}Si MAS NMR) analysis 29
2.3.10 Electron paramagnetic resonance analysis (EPR) 30
2.3.11 Thermogravimetric-Fourier transform-infrared (TGA-FT-IR) analysis 30
2.3.12 Determination of acidity of the catalysts (FT-IR of pyridine adsorption) 30
2.4 Catalytic activity studies 31
2.4.1 Gas chromatography analysis 33
2.4.2 Gas chromatography-mass spectra analysis 34
2.4.3 Calculation of the conversion (%) and the selectivity (%) 35

Chapter 3 – Results and Discussion - Catalysts Characterization

3.1 Powder X-ray diffraction (XRD) pattern 36
3.2 Fourier transform-infrared spectra (FT-IR) 38
3.3 Nitrogen adsorption-desorption analysis 42
3.4 Elemental analyses (AAS and EDX) 48
3.5 SEM and TEM studies 50
3.6 Diffuse reflectance UV-Vis spectra (DR UV-Vis) 54

3.7 Solid state ^{29}Si MAS NMR spectra analysis 55

3.8 Electron paramagnetic resonance spectra (EPR) analysis 59

3.9 Thermogravimetric-Fourier transform-infrared (TGA-FT-IR) analysis 61

3.10 Acidity of the catalysts (FT-IR of pyridine adsorption) 63

3.11 Conclusion 66

Chapter 4 – Results and Discussion - Catalytic Activity

4.1 Benzoylation of *p*-xylene 67

4.1.1 Introduction 67

4.1.2 Effect of various iron loadings 70

4.1.3 Effect of catalyst mass 72

4.1.4 Effect of benzoyl chloride to *p*-xylene molar ratio 73

4.1.5 Effect of reaction temperature 74

4.1.6 Effect of catalyst type 76

4.1.7 Comparison of the catalytic activity of RHA-10Fe, RHA-10Fe(Cal) and $Fe(NO_3)_3.9H_2O$ 78

4.1.8 Reaction kinetics 79

4.1.9 Reusability studies 82

4.1.10 Leaching study 83

4.1.11 Proposed reaction mechanism 84

4.2 Benzoylation of anisole 86

4.2.1 Introduction 86

4.2.2 Effect of iron loadings 90

4.2.3 Effect of catalyst mass 91

4.2.4 Effect of benzoyl chloride to anisole molar ratio 92

4.2.5 The effect of reaction temperature 94

4.2.6 Effect of catalyst type 96

4.2.7 Comparison of the reactivity of RHA-10Fe, RHA-10Fe(Cal) and $Fe(NO_3)_3.9H_2O$ as catalyst 97

4.2.8 Reaction kinetics 99

4.2.9 Leaching study 101

4.2.10 Reusability studies 103

4.2.11 Proposed reaction mechanism 105

4.3 Benzoylation of toluene 107

4.3.1 Introduction 107

4.3.2 Effect of iron loadings 110

4.3.3 Effect of catalyst mass 112

4.3.4 Effect of benzoyl chloride to toluene molar ratio 113

4.3.5 Effect of reaction temperature 115

4.3.6 Effect of catalyst type 117

4.3.7 Comparison of the catalytic activity of RHA-10Fe, RHA-10Fe(Cal) and $Fe(NO_3)_3.9H_2O$ 118

4.3.8 Reaction kinetics 120

4.3.9 Leaching test 123

4.3.10 Reusability studies 124

4.3.11 Proposed reaction mechanism 126

4.4 Conclusion 127

Chapter 5 – Conclusions and Recommendations

5.1 Conclusions 130

5.2 Recommendations 132

References 134

Appendices 151

List of publications and presentations in conferences 187

LIST OF TABLES

		Page
Table 2.1	GC programmes for benzoylation of *p*-xylene, anisole and toluene.	34
Table 2.2	GC-MS programmes for benzoylation of *p*-xylene, anisole and toluene.	34
Table 3.1	The N_2 adsorption-desorption analysis data for pure silica and metal incorporated silica samples.	47
Table 3.2	The average metal content (w/w)% obtained by EDX and AAS of the prepared catalysts.	49
Table 4.1	Effect of catalyst mass on the benzoylation of *p*-xylene.	72
Table 4.2	Benzoylation of *p*-xylene over different catalysts.	76
Table 4.3	The benzoylation of *p*-xylene over heterogeneous RHA-10Fe, RHA-10Fe(Cal) and homogeneous iron nitrate salt.	78
Table 4.4	Kinetic parameters for the benzoylation of *p*-xylene over RHA-10Fe at different temperatures.	80
Table 4.5	Reusability studies of RHA-10Fe.	82
Table 4.6	The leaching effect over RHA-10Fe during the *p*-xylene benzoylation.	83
Table 4.7	Effect of catalyst mass on the benzoylation of anisole.	92
Table 4.8	Benzoylation of anisole over different catalysts.	96
Table 4.9	Kinetic parameters for the benzoylation of anisole over RHA-10Fe at different temperatures.	100
Table 4.10	Effect of leaching over RHA-10Fe.	102
Table 4.11	Reusability of RHA-10Fe.	103
Table 4.12	Reusability of RHA-10Fe(Cal).	104
Table 4.13	Effect of catalyst mass on the benzoylation of toluene.	113
Table 4.14	Benzoylation of toluene over different catalysts.	117

Table 4.15	Kinetic parameters for the benzoylation of toluene over RHA-10Fe at various reaction temperatures.	121
Table 4.16	Effect of leaching of RHA-10Fe.	123
Table 4.17	Reusability of the as-synthesized RHA-10Fe.	124
Table 4.18	Reusability of the calcined RHA-10Fe(Cal).	125

LIST OF FIGURES

		Page
Figure 2.1	Typical liquid phase experimental set-up for benzoylation reaction.	31
Figure 3.1	The powder X-ray diffraction patterns of RHA-SiO_2, RHA-10Cu, RHA-10Sn and RHA-10Fe.	36
Figure 3.2	The powder X-ray diffraction patterns of RHA-5Fe, RHA-10Fe, RHA-15Fe and RHA-20Fe.	37
Figure 3.3	The powder X-ray diffraction patterns of RHA-10Fe and RHA-10Fe(Cal).	38
Figure 3.4	The FT-IR spectra of RHA-SiO_2, RHA-10Cu, RHA-10Sn and RHA-10Fe.	39
Figure 3.5	The FT-IR spectra of RHA-5Fe, RHA-10Fe, RHA-15Fe and RHA-20Fe.	40
Figure 3.6	The FT-IR spectra of RHA-10Fe and RHA-10Fe(Cal).	42
Figure 3.7	N_2 adsorption-desorption isotherms and BJH desorption pore size distribution (inset) of (a) RHA-SiO_2, (b) RHA-10Cu, (c) RHA-10Sn and (d) RHA-10Fe.	43
Figure 3.8	N_2 adsorption-desorption isotherms and BJH pore size distribution of (a) RHA-5Fe, (b) RHA-10Fe, (c) RHA-15Fe, (d) RHA-20Fe and (e) RHA-10Fe(Cal).	45
Figure 3.9	The SEM micrographs of (a) RHA-SiO_2 (× 20 K), (b) RHA-10Cu (× 20 K), (c) RHA-10Sn (× 30 K) and (d) RHA-10Fe (× 20 K).	51
Figure 3.10	The SEM micrographs of (a) RHA-5Fe, (b) RHA-10Fe, (c) RHA-15Fe, (d) RHA-20Fe and (e) RHA-10Fe(Cal) at 20 K magnification.	52
Figure 3.11	TEM micrographs of (a) RHA-SiO_2 and (b) RHA-10Cu.	53
Figure 3.12	The DR UV/Vis spectra of RHA-5Fe, RHA-10Fe, RHA-15Fe, RHA-20Fe and RHA-10Fe(Cal).	54
Figure 3.13	The DR UV/Vis spectrum of RHA-10Cu.	55

Figure 3.14	Different silicate Q-units.	56
Figure 3.15	The solid state ^{29}Si MAS NMR spectra of (a) RHA-SiO_2 and (b) RHA-10Cu.	56
Figure 3.16	The solid state ^{29}Si MAS NMR spectra of (a) RHA-5Fe and (b) RHA-10Fe. (* indicates spinning side bands)	57
Figure 3.17	EPR spectra of (a) RHA-5Fe (b) RHA-10Fe (c) RHA-15Fe (d) RHA-20Fe and (e) RHA-10Fe(Cal) at room temperature.	59
Figure 3.18	The TG and DTG curves of RHA-10Fe.	61
Figure 3.19	FT-IR spectra of gases evolved during decomposition of RHA-10Fe with library matching.	62
Figure 3.20	The FT-IR spectra of RHA-SiO_2, RHA-10Cu, RHA-10Sn and RHA-10Fe after pyridine adsorption.	64
Figure 3.21	The FT-IR spectra of pyridine adsorbed RHA-5Fe, RHA-10Fe, RHA-15Fe, RHA-20Fe and RHA-10Fe(Cal).	65
Figure 4.1	Effect of various iron incorporated catalysts in the benzoylation of *p*-xylene.	71
Figure 4.2	Effect of molar ratio of BzCl:*p*-xyl on the benzoylation of *p*-xylene.	73
Figure 4.3	The effect of reaction temperature on (a) The conversion of BzCl and (b) The selectivity to 2,5-DMBP.	75
Figure 4.4	Arrhenius plot for the benzoylation of *p*-xylene over RHA-10Fe at different reaction temperatures.	81
Figure 4.5	The proposed reaction mechanism for the benzoylation of *p*-xylene over Lewis acid sites in RHA-10Fe with minor contribution from Brønsted acid sites.	85
Figure 4.6	The effect of iron loadings on (a) The conversion of BzCl and (b) The selectivity towards *o*- and *p*-MOBP.	90
Figure 4.7	The effect of molar ratio of BzCl:Ani on (a) The conversion of BzCl and (b) The selectivity towards *o*- and *p*-MOBP.	93
Figure 4.8	The effect of reaction temperature on (a) The conversion of BzCl and (b) The selectivity towards *o*- and *p*-MOBP.	95
Figure 4.9	The benzoylation of anisole over homogeneous iron nitrate salt and heterogeneous RHA-10Fe, RHA-10Fe(Cal).	98

Figure 4.10	Arrhenius plot for the benzoylation of anisole over RHA-10Fe at different reaction temperatures.	101
Figure 4.11	The proposed reaction mechanism for the benzoylation of anisole over Lewis acid sites in RHA-10Fe with minor contribution from Brønsted acid sites.	106
Figure 4.12	The effect of metal loadings on (a) The conversion of BzCl and (b) The products selectivity towards *o*- , *m*- and *p*-MBP.	111
Figure 4.13	The effect of molar ratio of BzCl:Tol on (a) The conversion of BzCl and (b) The selectivity towards *o*- , *m*- and *p*-MBP.	114
Figure 4.14	The effect of reaction temperature on (a) The conversion of BzCl (b) The selectivity towards *o*-, m- and *p*-MBP.	116
Figure 4.15	The benzoylation of toluene over heterogeneous RHA-10Fe, RHA-10Fe(Cal) and homogeneous iron nitrate salt (a) The conversion of BzCl and (b) The selectivity towards *o*- , *m*- and *p*-MBP.	119
Figure 4.16	Arrhenius plot for the benzoylation of toluene over RHA-10Fe at different reaction temperatures.	122
Figure 4.17	The proposed reaction mechanism for the benzoylation of toluene over Lewis acid sites in RHA-10Fe with minor contribution from Brønsted acid sites.	127

LIST OF SCHEMES

		Page
Scheme 1.1	Friedel-Crafts acylation reaction: (Z)–Ar–H = aromatic compound; (Z) = substituent group(s); R–CO–X = acylating agent; R = alkyl or phenyl group; X = Cl, Br, I, RCOO or OH.	14
Scheme 4.1	Benzoylation of *p*-xylene with BzCl over the prepared catalysts.	70
Scheme 4.2	The benzoylation of anisole with BzCl over the prepared catalysts.	89
Scheme 4.3	Benzoylation of toluene with BzCl over the prepared catalysts.	110

LIST OF ABBREVIATIONS

Ani	Anisole
BA	Benzoic Acid
BAN	Benzoic Anhydride
BET	Brunauer, Emmett and Teller
BJH	Barret, Joyner and Halenda
BzCl	Benzoyl chloride
DR UV-Vis	Diffuse Reflectance Ultraviolet/Visible
EDX	Energy Dispersive X-ray analysis
EPR	Electron Paramagnetic Resonance
FT-IR	Fourier Transform Infra-Red
IUPAC	International Union of Pure and Applied Chemistry
m-MBP	*m*-Methylbenzophenone
o-MBP	*o*-Methylbenzophenone
o-MOBP	*o*-Methoxybenzophenone
p-MBP	*p*-Methylbenzophenone
p-MOBP	*p*-Methoxybenzophenone
p-xyl	*p*-Xylene
RH	Rice husk
RHA	Rice husk ash
RHA-10Cu	Copper (10 wt.%) incorporated silica from rice husk ash
RHA-10Fe	Iron (10 wt.%) incorporated silica from rice husk ash
RHA-10Fe(Cal)	RHA-10Fe calcined at 500 ^{o}C for 5 h.
RHA-10Sn	Tin (10 wt.%) incorporated silica from rice husk ash

RHA-15Fe	Iron (15 wt.%) incorporated silica from rice husk ash
RHA-20Fe	Iron (20 wt.%) incorporated silica from rice husk ash
RHA-5Fe	Iron (5 wt.%) incorporated silica from rice husk ash
RHA-SiO_2	Silica extracted from rice husk ash
SEM	Scanning Electron Microscopy
Si-OH	Silanol
Si-O-Si	Siloxane
TEM	Transmission Electron Microscopy
TGA-FT-IR	Thermogravimetric Analysis-Fourier Transform-Infrared
Tol	Toluene
USY zeolite	Ultra stable Y zeolite
XRD	X-Ray Diffraction
($[C_2dmim]^+$)	1-ethyl-2,3-dimethylimidazolium
($[C_8py]^+$)	*N*-octylpyridinium
($[C_nmim]^+$)	1-alkyl-3-methylimidazolium
($[NTf_2]^-$)	Bis(trifluoromethanesulphonl)imide
2,4-DMBP	2,4-Dimethylbenzophenone
2,5-DMBP	2,5-Dimethylbenzophenone
^{29}Si MAS NMR	Solid state ^{29}Si Magic Angle Spinning Nuclear Magnetic Resonance

LIST OF SYMBOLS

A	Frequency factor of Arrhenius constant
Å	Angstrom (=10^{-10} meters)
E_a	Activation energy
K	Kelvin (absolute temperature unit)
k	Reaction rate constant
k_a	The pseudo-first order rate constant
M	Molarity
nm	Nanometer (=10^{-9} meters)
P	Vapor pressure of gas at sample temperature (mm Hg)
P/P_0	Relative pressure
P_0	Absolute pressure inside sample chamber (mm Hg)
R	Universal gas constant, 1.987 cal mol^{-1} K^{-1}
T	Temperature
t	The reaction time
t_0	The reaction induction period
X	The fractional conversion of benzoyl chloride
ºC	Celcius (degree temperature unit)
%	Percentage

LIST OF APPENDICES

		Page
Appendix A	Energy dispersive x-ray analysis (EDX)	
Figure A1	EDX analysis data of RHA-SiO_2.	151
Figure A2	EDX analysis data of RHA-10Cu.	152
Figure A3	EDX analysis data of RHA-10Sn.	153
Figure A4	EDX analysis data of RHA-5Fe.	154
Figure A5	EDX analysis data of RHA-10Fe.	155
Figure A6	EDX analysis data of RHA-15Fe.	156
Figure A7	EDX analysis data of RHA-20Fe.	157
Figure A8	EDX analysis data of RHA-10Fe(Cal).	158
Appendix B	Transmission electron microscopy (TEM)	
Figure B1	TEM micrographs of (a) RHA-10Sn (b) RHA-5Fe (c) RHA-10Fe (d) RHA-15Fe (e) RHA-20Fe and (f) RHA-10Fe(Cal).	159
Appendix C	Solid state ^{29}Si MAS NMR data	
Figure C1	The solid state ^{29}Si MAS NMR spectra of (a) RHA-15Fe, (b) RHA-20Fe and (c) RHA-10Fe(Cal). (* indicates spinning side bands)	160
Appendix D	Thermogravimetric analysis- Fourier transform-infrared (TGA-FT-IR) spectroscopy data	
Figure D1(a)	The TG and DTG curves for RHA-SiO_2.	161
Figure D1(b)	FT-IR spectra of gases evolved during decomposition of RHA-SiO_2 with library matching.	161
Figure D2(a)	The TG and DTG curves for RHA-5Fe.	162
Figure D2(b)	FT-IR spectra of gases evolved during decomposition of RHA-5Fe with library matching.	162

Figure D3(a)	The TG and DTG curves for RHA-10Fe.	163
Figure D3(b)	FT-IR spectra of gases evolved during decomposition of RHA-10Fe with library matching.	163
Figure D4(a)	The TG and DTG curves for RHA-15Fe.	164
Figure D4(b)	FT-IR spectra of gases evolved during decomposition of RHA-15Fe with library matching.	164
Figure D5(a)	The TG and DTG curves for RHA-20Fe.	165
Figure D5(b)	FT-IR spectra of gases evolved during decomposition of RHA-20Fe with library matching.	165
Figure D6(a)	The TG and DTG curves for RHA-10Fe(Cal).	166
Figure D6(b)	FT-IR spectra of gases evolved during decomposition of RHA-10Fe(Cal) with library matching.	166
Figure D7(a)	The TG and DTG curves for RHA-10Cu.	167
Figure D7(b)	FT-IR spectra of gases evolved during decomposition of RHA-10Cu with library matching.	167
Figure D8(a)	The TG and DTG curves for RHA-10Sn.	168
Figure D8(b)	FT-IR spectra of gases evolved during decomposition of RHA-10Sn with library matching.	168
Appendix E	GC analysis data for benzoylation of *p*-xylene	
Figure E1	GC chromatogram for the benzoylation of *p*-xylene over RHA-10Fe.	169
Figure E2	GC chromatogram for the benzoylation of *p*-xylene over RHA-10Fe(Cal).	169
Figure E3	GC chromatogram for the benzoylation of *p*-xylene over RHA-10Sn.	169
Figure E4	GC chromatogram for the benzoylation of *p*-xylene over RHA-10Cu.	170
Figure E5	GC chromatogram for the benzoylation of *p*-xylene over iron nitrate salt.	170

Appendix F	GC analysis data for benzoylation of anisole	
Figure F1	GC chromatogram for the benzoylation of anisole over RHA-10Fe.	171
Figure F2	GC chromatogram for the benzoylation of anisole over RHA-10Fe(Cal).	171
Figure F3	GC chromatogram for the benzoylation of anisole over RHA-10Sn.	171
Figure F4	GC chromatogram for the benzoylation of anisole over RHA-10Cu.	172
Figure F5	GC chromatogram for the benzoylation of anisole over iron nitrate salt.	172
Appendix G	GC analysis data for benzoylation of toluene	
Figure G1	GC chromatogram for the benzoylation of toluene over RHA-10Fe.	173
Figure G2	GC chromatogram for the benzoylation of toluene over RHA-10Fe(Cal).	173
Figure G3	GC chromatogram for the benzoylation of toluene over RHA-10Sn.	173
Figure G4	GC chromatogram for the benzoylation of toluene over RHA-10Cu.	174
Figure G5	GC chromatogram for the benzoylation of toluene over iron nitrate salt.	174
Appendix H	GC-MS analysis data for benzoylation of *p*-xylene	
Figure H1	GC chromatogram for the products of benzoylation of *p*-xylene.	175
Figure H2	The mass spectrum of benzoic acid.	175
Figure H3	The mass spectrum of 2,5-dimethylbenzophenone.	176
Figure H4	The mass spectrum of 2,4-dimethylbenzophenone.	176
Figure H5	The mass spectrum of benzoic anhydride.	176

Appendix I	GC-MS analysis data for benzoylation of anisole	
Figure I1	GC chromatogram for the products of benzoylation of anisole.	177
Figure I2	The mass spectrum of benzoic acid.	177
Figure I3	The mass spectrum of *o*-methoxybenzophenone.	178
Figure I4	The mass spectrum of benzoic anhydride.	178
Figure I5	The mass spectrum of *p*-methoxybenzophenone.	178
Appendix J	GC-MS analysis data for benzoylation of toluene	
Figure J1	GC chromatogram for the products of benzoylation of toluene.	179
Figure J2	The mass spectrum of benzoic acid.	179
Figure J3	The mass spectrum of *o*-methylbenzophenone.	179
Figure J4	The mass spectrum of *m*-methylbenzophenone.	180
Figure J5	The mass spectrum of *p*-methylbenzophenone.	180
Figure J6	The mass spectrum of benzoic anhydride.	180
Appendix K	Kinetics study data for benzoylation of *p*-xylene, anisole and toluene	
Figure K1	Pseudo-first order plots for the benzoylation of *p*-xylene over RHA-10Fe at (a) 353 K, (b) 373 K, (c) 393 K and (d) 413 K.	181
Figure K2	Pseudo-first order plots for the benzoylation of anisole over RHA-10Fe at (a) 353 K, (b) 363 K, (c) 373 K and (d) 383 K.	182
Figure K3	Pseudo-first order plots for the benzoylation of toluene over RHA-10Fe at (a) 353 K, (b) 363 K, (c) 373 K and (d) 383 K.	183
Appendix L	Derivation of pseudo-first order equation	184

FERUM, KUPRUM DAN STANUM DISOKONG SILIKA ABU SEKAM PADI: PENYEDIAAN, PENCIRIAN DAN KEGUNAANNYA SEBAGAI MANGKIN UNTUK TINDAK BALAS BENZOILASI FRIEDEL-CRAFTS

ABSTRAK

Mangkin ferum, kuprum dan stanum disokong silika disediakan melalui kaedah sol-gel menggunakan silika yang diekstrak daripada abu sekam padi. Mangkin yang terhasil dilabel sebagai RHA-xFe (x = 5, 10, 15 dan 20 wt.%), RHA-10Cu dan RHA-10Sn. Mangkin-mangkin ini dicirikan menggunakan teknik fizikal-kimia seperti XRD, FT-IR, penjerapan-N_2, AAS, SEM-EDX, TEM, DR UV-Vis, ^{29}Si MAS NMR, EPR, TGA-FT-IR dan penjerapan piridin-FT-IR. Mangkin-mangkin ini didapati bersifat amorfus. Analisis unsur mengesahkan kehadiran logam dalam kekisi silika. Kajian keasidan pada mangkin dengan menggunakan kaedah jerapan FT-IR-piridin menunjukkan bahawa, tidak ada tapak asid Brønsted. Namun, ia mengandungi tapak asid Lewis. Aktiviti mangkin, RHA-xFe dengan muatan ferum berbeza telah dikaji untuk benzoilasi *p*-xilena, anisol dan toluena dalam fasa-cecair, dengan benzoil klorida sebagai agen pembenzoilasi. Kesan untuk pelbagai pemboleh ubah tindak balas seperti muatan ferum, jisim mangkin, perkadaran molar reaktan, suhu tindak balas, jenis mangkin, larut-lesap logam dan penggunaan semula mangkin turut dibincang. RHA-10Fe didapati sebagai mangkin paling efisien dari segi penukaran dan selektiviti. Perbandingan aktiviti pemangkinan RHA-10Fe, RHA-10Sn dan RHA-10Cu dalam tindak balas benzoilasi sebatian aromatik pada keadaan optimum tindak balas didapati mengikut urutan: RHA-10Fe >> RHA-10Sn > RHA-10Cu. Namun, keselektifan hasil didapati mengikut urutan: RHA-10Fe >> RHA-10Cu > RHA-10Sn untuk benzoilasi *p*-xilena dan toluena, manakala untuk benzoilosi anisol

adalah mengikut urutan: RHA-10Fe >> RHA-10Sn > RHA-10Cu. Garam homogen ferum ($Fe(NO_3)_3.9H_2O$) menunjukkan aktiviti lebih tinggi berbanding mangkin heterogen (RHA-10Fe dan RHA-10Fe(Cal)). Manakala selektiviti tertinggi terhadap produk yang diingini dicapai menggunakan RHA-10Fe(Cal) dalam tindak balas benzoilasi. Pengurangan dalam aktiviti pemangkinan diperhati apabila mangkin digunakan semula, yang boleh dikaitkan dengan larut-lesap sebahagian daripada tapak aktif ferum semasa tindak balas. Pengkalsinan mangkin mengurangkan larut-lesap logam dan meningkatkan penggunaan semula mangkin. Kajian kinetik bagi benzoilasi sebatian aromatik ke atas RHA-10Fe didapati mengikut tertib pseudo pertama. Satu mekanisme telah dicadangkan untuk laluan pemangkinan keatas mangkin yang disediakan.

IRON, COPPER AND TIN INCORPORATED RICE HUSK ASH SILICA: PREPARATION, CHARACTERIZATION AND APPLICATION AS CATALYSTS FOR FRIEDEL-CRAFTS BENZOYLATION REACTIONS

ABSTRACT

Iron, copper and tin incorporated silica catalysts were prepared via sol-gel method using the silica extracted from rice husk ash. The modified catalysts were denoted as RHA-xFe (x = 5, 10, 15 and 20 wt.%), RHA-10Cu and RHA-10Sn. Prepared catalysts were characterized by various physico-chemical techniques such as XRD, FT-IR, N_2-sorption, AAS, SEM-EDX, TEM, DR UV/Vis, solid state ^{29}Si MAS NMR, EPR, TGA-FT-IR and FT-IR-pyridine adsorption. The catalysts were found to be amorphous. Elemental analysis confirmed the presence of the metals in the silica framework. The acidity studies on the catalysts by using FT-IR-pyridine adsorption demonstrated that, there is no Brønsted acid sites. However, it has mainly Lewis acid sites. The catalytic activity of RHA-xFe with different iron loadings was studied for liquid-phase benzoylation of *p*-xylene, anisole and toluene with benzoyl chloride as benzoylating agent. The effect of various reaction parameters such as iron loadings, catalyst mass, molar ratio of the reactants, reaction temperature, catalyst type, leaching of metal and catalyst reusability was discussed. Compared to other iron loadings, RHA-10Fe was found to be the most efficient catalyst in terms of conversion and selectivity. Comparison of catalytic activity of RHA-10Fe, RHA-10Cu and RHA-10Sn in the benzoylation reaction of the aromatic compounds under the optimized reaction conditions was found to be in the order: RHA-10Fe >> RHA-10Sn > RHA-10Cu. However, the products selectivity followed the order: RHA-10Fe >> RHA-10Cu > RHA-10Sn for the benzoylation of *p*-xylene and toluene,

while for the benzoylation of anisole as in the order: RHA-10Fe >> RHA-10Sn > RHA-10Cu. The homogeneous iron salt ($Fe(NO_3)_3.9H_2O$) was tested for the reaction under the optimized conditions, and it showed higher activity over the heterogeneous catalysts (RHA-10Fe and RHA-10Fe(Cal)), whereas the highest desired product selectivity was obtained using RHA-10Fe(Cal) in the benzoylation reaction. Upon reuse of the catalyst, some decrease in the activity was observed, which can be related to leaching of some active iron sites during the reaction. The calcination of the catalyst reduced the leaching of the iron and improved the reusability. The kinetic study of the benzoylation of the aromatic compounds over RHA-10Fe was found to follow a pseudo-first order rate law. A mechanism was proposed for the catalytic pathways over the prepared catalysts.

Introduction

1.1 General introduction

Malaysia is one of the rice producing countries in the world. The annual production of rice leaves behind about 3.6 million tons of husk as a waste product (Rahman *et al.*, 1997). It is usually disposed by combustion giving *ca.* 20% of rice husk ash (RHA). Unfortunately, this RHA residue left after the combustion causes environmental problems (Rahman *et al.*, 1997; Chandrasekhar *et al.*, 2003). However, RHA can be employed as raw materials in a variety of applications such as pozzolan in cement and concrete (Siddique, 2008). The chemical analysis of RHA shows that it contains 90-97% of silica, which can exist either in amorphous phase or in crystalline phase. The recovery of amorphous silica from RH is considered to be the cheapest alternative source of silica due to the presence of abundant source of rice husk around the country. Further, since the ash is obtained as a fine powder, it does not require more grinding and thus, making it the most economical source for nanoscale silica (Liou, 2004).

By using RHA as the silica source in the preparation of the catalysts the production costs can be reduced substantially besides helping to overcome environmental pollution. Indeed, utilization of silica as a support for the preparation of the catalyst via a sol-gel process promises several advantages such as it allows a better control over the texture, homogeneity, composition and the structural properties of the catalysts. Other advantages are, lower temperature, high yield, short processing time, cost effectiveness and environment friendly (Campanati *et al.*, 2003).

Acylation of aromatic compounds to prepare aromatic ketones is of commercial importance in various areas of the fine chemical and pharmaceutical industry. In the Friedel-Crafts acylation, an aromatic ketone is prepared by the reaction of an aromatic compound with an acylating agent in the presence of an acid catalyst (Jasra, 2003). Metal halides such as $AlCl_3$ and protonic acids like H_2SO_4 and anhydrous HF are used as acid catalysts (Olah, 1963). However, these conventional catalysts have drawbacks in terms of a requirement of more than stoichiometric quantities, non-regeneratable, require further treatment after reaction, produce large amounts of hazardous corrosive waste and catalyze undesirable side reactions (Smith *et al.*, 1998; Jacob *et al.*, 1999). Therefore, the demand for fewer pollutants and a more effective chemical process has become the current concern.

In recent years, the drive towards cleaner and safer production methods and higher selectivities has given industry the impetus to change some of the Friedel-Crafts processes in favor of catalysts featuring higher selectivities and easier handling. A number of heterogeneous solid catalysts based on zeolites, metal oxides, clays, heteropoly acids, sulphated zirconia and mesoporous silica have been reviewed for Friedel-Crafts acylation reactions (Sartori and Maggi, 2006; Jana, 2006).

In this study, heterogeneous catalysts were prepared by using silica from rice husk ash as support for some metals, namely, iron, copper and tin at room temperature via a sol-gel method. The prepared catalysts were characterized using different techniques, e.g. elemental analysis, textural analysis, surface analysis, and spectroscopic analysis. The activity of these catalysts was tested for the Friedel-Crafts acylation reaction, i.e. benzoylation of *p*-xylene, anisole and toluene. The

reaction conditions were optimized for these reactions with the prepared catalytic systems, and their kinetics were studied.

1.2 Rice husk (RH)

Rice husk (RH) is the milling by-product of rice, a major food material in rice producing countries, including Malaysia. It is a major agriculture waste material produced in significant quantities on a global basis. It has been reported that Malaysia produces 18 million tons of paddy rice that leaves behind about 3.6 million tons of husk as a waste product (Rahman *et al.*, 1997). However, RH has little or no commercial application. It is usually either burned or discarded, resulting not only in resource wasting, but also in environmental pollution (Usmani *et al.*, 1994; Chang *et al.*, 2006). Therefore, for both industrial and environmental purposes, it makes sense to try and utilize the RH. Researches are being carried out to overcome this problem, which includes generating valuable products from this waste material. As such the utilization of RH will not only reduce the pollution problem caused by the ash but also produce value added products from the economic perspective.

1.2.1 Properties and chemical composition of rice husk

RH is a thin but abrasive skin covering the edible rice kernel. The major constituents of rice husk are cellulose, lignin and silica ash (Yal□in and Sevin□, 2001). The chemical constituents in RH are found to vary from sample to sample, which may be due to the different geographical conditions, type of paddy, climatic variation, soil chemistry and fertilizers used in the paddy growth (Chandrasekhar *et al.*, 2005). RH consists of organic and inorganic elements. Chandrasekhar *et al.* (2003) reported that the organic content in RH was 72% of the husk by weight. The

actual chemical composition of RH is variable, typically: ash 20%, lignin 22%, cellulose 38%, pentosans 18%, and other organics 2% (Chandrasekhar *et al.*, 2003; Adam and Chua, 2004). The silica content in the ash was found to be more than 90–97% (Mansaray and Ghaly, 1997) with a small proportion of metallic elements.

1.2.2 Rice husk ash (RHA)

Rice husk ash (RHA) is produced by burning the husks of a rice paddy. On burning, cellulose and lignin are removed leaving behind silica ash. The controlled temperature and environment of burning yields better quality rice husk ash as its particle size and specific surface area are dependent on the burning conditions (Siddique, 2008).

The physical properties of RHA largely depend on the burning condition. Particularly, the time and temperature of burning affect the structure and characteristics of RHA (Della *et al.*, 2002). The partial burning of rice husks produces black RHA, whereas the complete burning results in either white or grey RHA (Ismail and Waliuddin, 1996). In addition, the burning at a high temperature (more than 800 °C) produces crystalline silica of α-cristobalite and tridymite (Siddique, 2008). While the controlled burning at 500 to 800 °C results in non-crystalline or amorphous silica, which is highly reactive due to its ultrafine size and high surface area, which can provide sufficient surface for any metal to disperse on it (Real *et al.*, 1996; Mekhemer *et al.*, 1999). Due to the fact that rice husk ash contains high silica content, it can be used as an economically viable material for silica gel and powder production (Kamath and Proctor, 1998).

1.2.3 Preparation and purity of silica from RHA

The presence of silica in rice husk has been known since 1938 (Chandrasekhar *et al.*, 2003; Radhika and Sugunan, 2006a), while its recovery potential had been realized since 1984 (Kaupp, 1984). It is considered as a good source of highly reactive silica.

To prepare high purity silica with a high specific surface area from rice husk, either direct combustion (Kapur, 1985; Luan and Chou, 1990; Della *et al.*, 2002) of the husk or treatment with various chemicals was attempted (Chakraverty *et al.*, 1988; Conradt *et al.*, 1992; Yal□in and Sevin□, 2001; Matori *et al.*, 2009) before and after combustion at temperatures ranging from 500 to 1400 °C for different intervals of time (Della *et al.*, 2002).

Quite a few kinds of acids (HCl, H_2SO_4, HNO_3 and HF) have been reported to be used in the pre-treatment (Mishra *et al.*, 1985; Patel *et al.*, 1987; Liou, 2004), but HCl is the most often used.

Chakraverty *et al.* (1988) found that the leaching of RH in dilute HCl (1 N) was effective in substantially removing most of the metallic impurities. Acid treatment of RH prior to combustion does not affect the amorphicity of the silica produced. After acid leaching, the silica produced was completely white in colour and had high purity (Chakraverty *et al.*, 1988).

Other acids, such as H_2SO_4, HNO_3 had also been used in acid pre-treatment (Patel *et al.*, 1987; Proctor, 1990; Ahmed and Adam, 2007). The general leaching effects of H_2SO_4, HNO_3 and HCl is similar, but HCl leaching of RH is superior to H_2SO_4 and HNO_3 in removing the metallic ingredients (Matori *et al.*, 2009).

Chemical treatment before combustion was found to be more advantageous because some metal oxides may contaminate the resulting silica. It has been found

that some kinds of metal oxides, especially K_2O, contained in RHA cause the formation of black particles in the silica from an untreated husk and also cause the surface melting of SiO_2 particles and accelerate the crystallization of amorphous SiO_2 into cristobalite (Proctor, 1990; Krishnarao, 2001; Chandrasekhar *et al.*, 2006). Real *et al.*, had reported this phenomena is due to the strong interaction between the silica and the K^+ contained in RH, which leads to a dramatic decrease of the specific surface area if K^+ cations were not removed before the heat treatment of the samples (Real *et al.*, 1996; Real *et al.*, 1997). Therefore, the main effect of acid leaching is to remove metal oxides, especially potassium oxides.

Some alkalis, such as NaOH and NH_4OH, have also been used to pre-treat RH (Patel *et al.*, 1987; Conradt *et al.*, 1992; Yal□in and Sevin□, 2001). However, the effects of alkali pre-treatment are not as obvious as the effects of acid pre-treatment.

Amorphous silica from RHA can be extracted using the sol-gel process at low temperature alkali extraction because the solubility of amorphous silica is very low at pH < 10 and increases sharply pH > 10 (Iler, 1979). This unique solubility behavior enables silica to be extracted in a pure form from RHA by solubilizing under alkaline conditions and subsequently precipitating at a lower pH (Kamath and Proctor, 1998). This simple and low energy method to produce silica by alkaline solubilization and subsequent acid treatment had been reported by Kamath and Proctor (1998) and Kalapathy *et al.* (2000a) to be the more economical process having the potential to replace the conventional high energy smelting processes (Iler, 1979; Brinker and Scherer, 1990). This is because thermal treatment of RH actually produces energy instead of consuming energy. The energy produced could be recovered in the form of heat or electricity.

Kalapathy *et al.* (2002) used an improved method to produce silica with lower sodium content by adding silicate solution to hydrochloric, citric or oxalic acid solutions until pH 4.0 were reached.

Ahmed and Adam (2007) studied the effect of different concentration of NaOH (1.0 , 3.0 and 5.0 M) in the preparation of the silica, and they found that the change in alkali concentration used during the preparation had only affected the porosity and pore structure of the prepared silica and did not affect the chemical environment.

1.2.4 Application of the silica extracted from RHA

Due to the high silica content of RHA, it can be used in many industrial and chemical applications such as filler, additive, vegetable oil refining, pharmaceutical products, detergents, adhesive agents, semiconductors, optical devices, glass, ceramics, cements, chromatography and production of porous materials (Proctor and Palaniappan, 1990; Fuad *et al.*, 1995; Padhi and Patnaik, 1995; Kalapathy *et al.*, 2000b; Chandrasekhar *et al.*, 2003).

Amorphous silica with high purity and reactivity is an excellent starting material for the synthesis of various fine chemicals such as silicon carbide, silicon nitride, magnesium silicide and high purity elemental silicon (Singh *et al.*, 1995; Sun and Gong, 2001; Martínez *et al.*, 2006). Furthermore, it is useful for the synthesis of different types of zeolites; zeolite beta (Prasetyoko *et al.*, 2006), zeolite A and Y (Hamdan *et al.*, 1997), zeolite ZSM-5 (Rawtani *et al.*, 1989) and zeolite ZSM-48 (Wang *et al.*, 1998).

Recently, the use of RHA as sources for the synthesis of mesoporous silica such as SBA-15, MCM-41 and MCM-48 has already been reported in the literature (Endud and Wong, 2007; Jang *et al.*, 2009; Bhagiyalakshmi *et al.*, 2010).

1.2.5 Applications of the silica as adsorbent and catalyst support

Properties like high surface area and porosity give added advantage to the silica for its use as adsorbents, catalysts and catalyst supports. RHA has been evaluated as an adsorbent of minor vegetable oil components (Proctor and Palaniappan, 1990; Proctor *et al.*, 1995). Proctor and Palaniappan (1990) have studied the ability of RHA to adsorb free fatty acid from soy oil. Adam and co-workers (Saleh and Adam, 1994; Adam and Ravendran, 2000) had shown that the adsorption of saturated fatty acid on RHA follows a Langmuir isotherm.

In another work, Adam and Chua (2004) studied the chemical incorporation of aluminium ions into RHA by the sol-gel technique and its adsorptive capability towards fatty acids. The RHA-Al was found to be a very good adsorbent for palmytic acid.

The application of silica as a catalyst support has been extensively studied to meet the demand for high surface area, high metal dispersion, high thermal stability, high melting point and high reactivity material (Radhika and Sugunan, 2006b). Instead of commonly used silica gel (SiO_2), Chang *et al.* (Chang *et al.*, 1997; Chang *et al.*, 2003a; Chang *et al.*, 2005) for the first time adopted rice husk ash (RHA) as a catalyst-support and found that nickel-loaded RHA exhibited a very high activity for CO_2 hydrogenation (Chang *et al.*, 2001; Chang *et al.*, 2003b). In all reported cases either the incipient wetness impregnation method or ion exchange methods were used to physically incorporate the metal ions into the rice husk silica matrix.

Consequently, preparation of catalysts utilizing RHA as a cheap source of silica is a very attractive alternative to the current use of tetraethyl orthosilicate (TEOS) as a starting material for most silica based catalysts. To date, several publications had been reported on the use of rice husk ash as a matrix for preparing metal supported heterogeneous catalysts for the Friedel-Crafts alkylation reaction of aromatics (Adam *et al.*, 2006; Adam and Andas, 2007; Adam and Ahmed, 2008; Ahmed and Adam, 2009) and for the oxidation reaction (Renu *et al.*, 2008; Adam *et al.*, 2009; Adam and Fook, 2009; Adam and Sugiarmawan, 2009).

Recently, we showed that chemical incorporation of iron into rice husk ash silica resulted in an excellent catalyst for the Friedel-Crafts benzylation of toluene, benzene and xylenes (Adam *et al.*, 2006; Adam and Ahmed, 2008; Ahmed and Adam, 2009).

Adam and Andas reported the synthesis of 4-(methylamino) benzoic acid incorporated iron-silica catalyst extracted from rice husk. This catalyst, (RHA-Fe (5%-amine)) was found to be more selective to mono benzyl toluene in the benzylation of toluene (Adam and Andas, 2007).

In all these previous reports, iron supported rice husk silica has been used as a catalyst for the Friedel-Crafts alkylation reaction. However, there is no published literature on iron loaded rice husk silica being used as a catalyst for the Friedel-Crafts acylation reaction.

1.3 Catalysis and catalyst

Catalysis is the key to chemical transformations. The most industrial syntheses and nearly all biological reactions require catalysts (Hagen, 2006). Furthermore, catalysis plays a fundamental role in the industries. Specifically, two of the largest industrial segments, chemicals and petroleum processing, depend on

catalysis; many of the modern, cost and energy-efficient environmental technologies are catalytic. Biocatalysis offers exciting opportunities for producing a broad range of pharmaceuticals and specialty chemicals, and for bioremediation of the environment (Nur, 2006).

Catalyst is defined as a substance that increases the rate of attainment of chemical equilibrium without itself undergoing chemical change (Thomas and Thomas, 1997). Catalyst increases the reaction rate by offering another route of reaction with lower activation energy of the reaction system. There are many chemical reactions including Friedel-Crafts acylation reactions, which need these catalysts in order to enhance the reaction rate. The presence of the catalyst is essential for (i) obtaining new products, (ii) increasing productivity, (iii) decreasing the raw materials and energy consumption, (iv) minimizing the waste production and safeguarding the environment (Barrault, *et al.*, 2002). Today, catalysts play a vital role in the chemical industries, with a total contribution of ~20% of world Gross National Product (GNP) in the 20th century (Clark, 2002). In addition, 80% of the industrial reactions such as acylation, oxidation, hydrogenation, epoxidation etc. use catalysts.

1.3.1 Classification of catalysts

The numerous catalysts known today can be classified according to structure, composition, area of application, or state of aggregation. According to state of aggregation, catalysts can be classified into two large groups: homogeneous and heterogeneous catalysts (Hagen, 2006). Homogeneous catalyst is referred as the catalyst that exists in the same phase with the reactants, e.g. $AlCl_3$ has been widely used as a homogeneous catalyst in the Friedel-Crafts acylation reaction (Olah and

Molnár, 2003), whereas heterogeneous catalyst is a catalyst which has a different phase with the reactants, e.g. zeolites, which are extensively employed in petroleum refinery processes (Weitkamp, 2000). Catalyst can be gas, liquid or solid. Most industrial catalysts are liquids or solids, whereby the latter react only via their surface (Hagen, 2006). According to Hagen, the heterogeneous catalysts can be divided into two parts: bulk catalysts and supported catalysts. In supported catalysts, the catalytically active substance is applied to a support material, which has a large surface area and is usually porous (Hagen, 2006).

Heterogeneous catalysis is the backbone of the modern chemical industry, because of the necessity to achieve environmental benign processes in the industry. Although heterogeneously catalyzed processes are widely used in large scale petrochemical processes, the majority of fine, speciality pharmaceutical chemicals manufacturing processes rely on homogeneous catalysts, with solid catalysts used in little beyond hydrogenations. Many of these processes were developed simply to maximize product yield, disregarding the environmental impact of the inorganic waste and toxic byproducts formed during the reaction. Most of the waste is generated during the separation stage of the process when a typical water quenched and neutralization (for acidic or alkaline systems) results in the formation of large volumes of hazardous waste (Clark, 2002). Therefore, the industries nowadays prefer to use solid heterogeneous catalyst compared with liquid homogeneous catalyst. In addition, heterogeneous catalysts offer numerous potential advantages over homogeneous catalysts, such as easier working up procedures, easy catalyst separation from the reaction mixture, reduction of environmental pollutants, avoidance of salt formation and waste disposals (Wilson and Clark, 2000). The use of microporous and mesoporous solid catalysts has shape selective properties, an

additional benefit in fine chemical synthesis. Furthermore, the modification of the solid catalysts by metals having redox functions along with acidic or basic properties extends their catalytic scope to redox reactions. Hence, the development of reusable solid catalysts having redox function along with their acidity or basicity for the liquid phase Friedel-Crafts acylation reactions is useful for the preparation of fine chemicals (Jana, 2006).

1.3.2 Supported catalysts

Supported catalysts consist of an active phase dispersed on a support. The catalytic reaction takes place on the surface (i.e. in the pores) of the catalyst. Good supports combine relatively high dispersion with a high degree of thermal stability of the catalytic component (Campanati *et al.,* 2003). There are a number of materials that partly or wholly satisfy these requirements and utilized as heterogeneous catalysts for Friedel-Crafts acylation reaction, including zeolites, metal oxide, heteropoly acids, clays, alumina and mesoporous materials (Clark, 2002; Sartori and Maggi, 2006).

The preparation of supported catalysts aligns all the unit operations toward dispersing an active agent on a support that may be inert or catalytically active. The wetting of the support with a solution or slurry of the active phase precursors is the operation that characterizes such a preparation. The other operations (drying, washing, calcination, forming) are ruled by the same laws, depend on the same parameters and use the same equipment. The most common preparation methods for supported catalysts are incipient wetness impregnation, ion-exchange, adsorption and deposition–precipitation (Perego and Villa, 1997). The sol-gel process can also be successfully applied for catalyst preparation (Brinker and Scherer, 1990; Gonzalez *et*

al., 1997). The sol-gel method has several promising advantages over precipitation method for preparing ultrafine, high purity, single and multicomponent oxide glasses and ceramic composites with the advantages of high purity, lower sintering temperature, a high degree of homogeneity, high yield, small processing time, cost effectiveness and environmental friendly (Naskar and Chatterjee, 2004; Chatterjee and Naskar, 2006). Sol-gel process offers better control over surface area, pore volume and pore size distribution of the catalysts (Perego and Villa, 1997; Campanati *et al.*, 2003).

In general, the sol-gel process involves the transition of a system from a liquid sol (mostly colloidal) into a solid gel phase. In a typical sol-gel process, the precursor is subjected to a series of reaction including hydrolysis, condensation, gelation, aging and drying to produce a gel (Vansant *et al.*, 1995). This route makes it possible to incorporate metals into various matrices (e.g. silica, alumina, etc.) with very small particle size and homogeneous distribution. The resulting materials are proven to be active catalysts in different reactions.

1.4 Friedel-Crafts reactions

Since its discovery in 1877 by Charles Friedel and James Mason Crafts, the Friedel-Crafts reactions have become the most common and important transformation in organic chemistry. It is widely used not only in research but also in chemical production industries (Olah, 1963). One of the best definitions for Friedel-Crafts reactions is given by Nobel Prize laureate G. A. Olah in the classical series 'Friedel-Crafts and Related Reactions' (Olah, 1963) in which he defines these reactions 'to be any substitution, isomerization, elimination, cracking, polymerization or addition reactions taking place under the catalytic effect of Lewis acid type acidic halides (with or without co-catalysts) or proton acids'.

Friedel-Crafts reactions are electrophilic in nature and can be divided into two main categories – alkylation and acylation. The essential feature of the reaction consists in the replacement of a hydrogen atom of an aromatic compound by an alkyl or acyl group derived from an alkylating or acylating agent in the presence of Lewis acids (e.g. $AlCl_3$, BF_3, $FeCl_3$, $ZnCl_2$, etc.) or protonic acids (e.g. H_2SO_4, HF, etc.). Among all the catalysts, $AlCl_3$ is commonly used as an extremely powerful catalyst for the Friedel-Crafts type reactions (Olah and Molnár, 2003).

1.4.1 Friedel-Crafts acylation

Friedel-Crafts type acylation of aromatic compounds is an important reaction used in the synthesis of aromatic ketones, which are important chemical intermediates in the pharmaceutical, fragrance, flavor, dye and agrochemical industries (Geneste and Finiels, 2006; Sartori and Maggi, 2006). For example, they are components in the synthesis of nonsteroidal anti-inflammatory drugs Ibuprofen and S-Naproxen (Andy *et al.*, 2000; Jasra, 2003). Friedel-Crafts acylation is an electrophilic aromatic substitution to afford ketones by replacing one of the hydrogen of an aromatic ring (Scheme 1.1). Carboxylic acids, acid halides and anhydrides, serve as acylating agents and Lewis acid metal halides are the characteristic catalysts required to induce the transformation (Olah and Molnár, 2003).

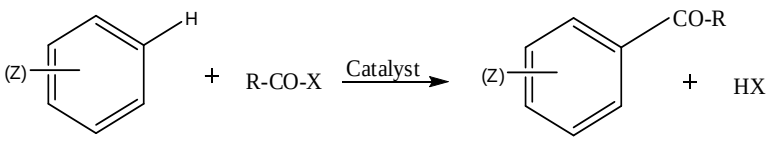

Scheme 1.1: Friedel-Crafts acylation reaction: (Z)–Ar–H = aromatic compound; (Z) = substituent group(s); R–CO–X = acylating agent; R = alkyl or phenyl group; X = Cl, Br, I, RCOO or OH.

1.4.2 The difference between Friedel-Crafts type acylation and alkylation reactions

Acylating agents in general are more reactive than alkylating agents in Friedel-Crafts type reactions. The reaction of acyl halides with aromatic compounds in the presence of Friedel-Crafts catalyst proceeds more readily than the corresponding alkylation with alkyl halides. Usually it is difficult to introduce more than one acyl group into an aromatic ring. This occurs because the deactivated nature of the acylated product is not further active in multiple acylation. Another significant difference is that more than stoichiometric amounts of the catalyst is required, compared with the catalytic quantity only that is required in the alkylation. This is due to the formation of complex between the catalyst and the carbonyl group of the ketone product. The electrophile in a Friedel-Crafts acylation is an acylium ion, which is stabilized by resonance and is not prone to rearrangement unlike Friedel-Crafts alkylation (Olah, 1963; Sykes, 1986; Olah and Molnár, 2003).

1.4.3 Homogeneously catalyzed acylation

$AlCl_3$ is a very active catalyst, and it is the most frequently used catalyst in aromatic Friedel-Crafts acylation, but other Lewis acid metal halide ($FeCl_3$, $SnCl_4$, $ZnCl_2$, etc.) also show high activity. Since the activity of Lewis acid metal halides depend on the reagents and reaction conditions, relative reactivity orders may be established for a given reagent only under given reaction conditions. Based on their activity in the acetylation with acetyl chloride of toluene, $SbCl_5$, $FeCl_3$, $SnCl_4$ and $TiCl_4$ are also efficient catalysts. Whereas $ZnCl_2$ is usually a relatively weak Lewis acid in Friedel-Crafts acylation and requires higher temperature (Gore, 1955; Olah and Molnár, 2003).

Boron trifluoride (BF_3) is another important, reactive Friedel-Crafts catalyst that has been widely used. Since BF_3 is a volatile gas it can form many complexes and can be readily recovered for reuse. For example, acylation of 2-methylnaphthalene with iso-BuCOF and BF_3 gives high yield (83%) of the 6-substituted isomer in contrast to $AlCl_3$ (30%) (Hyatt and Raynolds, 1984). Brønsted acids such as HF, H_2SO_4, H_3PO_3, etc., are also available to induce acylation. Perfluoroalkanesulfonic acids were shown to be highly effective. Certain metal powders, such as Zn, Cu, Al and Fe were also found to affect acylations with acyl chlorides (Gore, 1955). The use of homogeneous catalysts is recognized with a number of disadvantages. The major disadvantage of the above homogeneous catalysts is that more than a stoichiometric amount of the catalysts are needed due to the complex formation with the acylating agent as well as the carbonyl product. The intermediate complex is usually hydrolyzed with water and consequently, produces a large amount of waste products that cause serious technological and environmental problems (Gaare and Akporiaye, 1996; Smith *et al.*, 1998). Mild Lewis acids like rare earth triflates and bismuth(III) salts have been realized as catalysts, forming fewer stable complexes with the product, but achieved limited success (Métivier, 2001). In industrial processes, the reaction brings another disadvantage to this system where it has a difficulty in product purification due to the large amount of side products (Hu *et al.*, 2000). In addition, the inherent disadvantage of the use of these catalysts is non-regeneratable, low selectivity and generated hazardous corrosive waste products (Campanati *et al.*, 1998).

The quantity, handling, corrosive nature and disposal of the Lewis acids and the hazardous nature of mineral acids, led to environmental concerns that have

stimulated research aimed at the development of safer and non-waste producing alternatives based on heterogeneous solid acid catalysts.

1.4.4 Heterogeneously catalyzed acylation

Heterogeneous solid acid catalysts have certain advantages over the homogeneous ones. They offer easier separation and recovery of the products and catalyst from the reaction mixture. These are reusable, generally not corrosive and do not generate problematic side products. Additionally, they contribute shape selectivity to the product. Thus shape selective heterogeneous catalysts are very capable of replacing traditional homogeneous Friedel-Crafts catalysts (Jana, 2006). Different classes of materials have been studied and utilized as heterogeneous catalysts for Friedel-Crafts acylations.

The most common solid acids that have been studied are zeolites. Among the various types of zeolites, beta, Y, mordenite, MCM-22 and ZSM-5 are widely used for Friedel-Crafts acylation reactions (Pandey and Singh, 1997; Laidlaw *et al.*, 2001; Choudhary *et al.*, 2003; Singh and Venkatesan, 2003; Klisáková *et al.*, 2004). It is reported that, the activity of zeolite in the liquid-phase acylations largely depends on their structural features and the activity increases from medium to large pore and from mono to three dimensional channel systems (Klisáková *et al.*, 2004). Due to the above reasons, beta zeolite is found to be the best and the most suitable zeolite catalyst for Friedel-Crafts acylation of aromatics in comparison to the others. Unfortunately, the catalytic activity of microporous beta zeolite is restricted by their small pore sizes of around < 8 Å, which makes them unsuitable for reactions involving bulky substrates (Wilson and Clark, 2000; Jana, 2006).

However, recent developments in material chemistry have led to the discovery of the mesoporous molecular sieves family (Beck *et al.*, 1992) offering pore sizes in the range 20–100 Å which opens up new possibilities for liquid-phase acid catalysis by enabling rapid diffusion of reactants and products through the pores, thus minimizing consecutive reactions (Wilson and Clark, 2000). Choudhary *et al.* had reported the usage of mesoporous Si-MCM-41 and its modification by oxides and chlorides of gallium and indium as Lewis acids in Friedel-Crafts acylation of aromatics with acyl chloride (Choudhary *et al.*, 2000; Choudhary *et al.*, 2002; Choudhary and Jana, 2002b). MCM-41 has also been used for the acylation of various bulky aromatic compounds, e.g. naphthalene and substituted naphthalenes (Gunnewegh *et al.*, 1996; Choudhary and Jha, 2007).

The use of clays in the acylation of aromatics by acyl chloride as acylating agent is very limited in the literature. Montmorillonite K10 and KSF with or without modifications by Fe (III) and Zn (II) were reported for the acylation of activated aromatics by acyl halides (Cornélis *et al.*, 1990; Cornélis *et al.*, 1993; Choudary *et al.*, 1998). Bentonite clay supported polytrifluoromethanesulfosiloxane was also applied for the acylation of highly activated aromatic compound (ferrocene) with acyl chloride (Hu and Li, 2004). In addition, the use of clay based solid for the acylation of nonactivated aromatics, e.g. benzene by acyl halide was reported by Choudhary *et al.* (2001a).

Heteropolyacids (HPAs) are an interesting class of super acids. One important advantage of HPAs is that it can be utilized both homogeneously and heterogeneously depending on the nature of the solvent. Numerous reports exist on the use of HPAs based catalysts for acylation reactions. Kozhevnikov had reviewed the Friedel-Crafts acylation of arenes catalyzed by HPA-based solid acids

(Kozhevnikov, 2003). Kozhevnikov and coworkers reported efficient acylation of anisole with a bulk supported HPAs and Cs salt of HPA (Kaur *et al.*, 2002a; Kaur and Kozhevnikov, 2002b). It is well-known that one of the major problems associated with HPAs in the bulk form is its low efficiency due to low surface area, rapid deactivation, and relatively poor stability (Sartori and Maggi, 2006).

1.4.5 Green chemistry and solid acids

Solid acids are heterogeneous catalytic materials that are used in green chemistry applications. Green chemistry has a number of principles (Anastas *et al.*, 2000). Some of them are: (i) the prevention of chemical waste is better than a focus on cleanup or treatment of chemical waste after it is formed; (ii) encouraging economy/efficiency, in part by minimizing or eliminating solvents, separating agents, and protecting groups; (iii) reducing the toxicity of products and byproducts; (iv) the use of renewable raw material feedstocks; (v) searching for reactions that take place at room temperature and pressure in order to reduce energy consumption; and (vi) choosing substances that minimize the potential for chemical accidents.

Many of these green chemistry principles are directed at the development and utilization of solid acids. Solid acids can be used to replace corrosive and toxic Lewis and Brønsted acids, such as $AlCl_3$ and HF, which are presently used in large-scale chemical syntheses, thereby producing less waste and increasing the safety of the manufacturing process. In addition to replacing undesirable conventional acid reagents, solid acids have the advantages of being reusable, non-corrosive, highly selective, easily separable from reaction mixtures, and generating fewer hazardous byproducts (Macquarrie, 2000; Sartori and Maggi, 2006).

1.5 Scope of the thesis

Acylation of aromatic compounds is the main route for the formation of aromatic ketones, which are widely used in various areas of fine chemical and pharmaceutical industry. Recently, a few articles have been published by our group (Adam *et al.*, 2006; Adam and Andas, 2007; Adam and Ahmed, 2008; Ahmed and Adam, 2009) which showed that, iron incorporated rice husk silica was an efficient catalyst for the Friedel-Crafts alkylation reaction. However, literature review show that there are no reports on the catalytic activity of iron incorporated rice husk silica for the Friedel-Crafts acylation reactions, i.e. benzoylation of aromatic compounds. Hence it was thought interesting to study in detail the incorporation of various heteroatoms namely iron, copper and tin in the silica framework from rice husk ash and to evaluate its catalytic activity in the Friedel-Crafts benzoylation reactions of *p*-xylene, anisole and toluene.

Commercially, the starting materials for the production of most silica based catalysts are tetraethyl orthosilicate (TEOS) and tetramethyl orthosilicate (TMOS). However, the use of these organosilicon compounds requires high cost (Adam and Iqbal, 2010). In this present study, the use of the silica extracted from rice husk ash has been used in place of commercial silica. This will lower the cost of the catalyst production since rice husk can be obtained free of charge.

The work reported in this study focuses on the synthesis of RHA-xFe with different loadings using rice husk ash as a silica source at room temperature via sol-gel method. The modification with tin and copper was also studied in order to compare with the iron based catalysts.

Characterization of the prepared catalysts was carried out using Fourier Transform-Infrared (FT-IR) spectroscopy to study the functional groups while the

nature of the samples was analyzed by powder X-ray Diffraction analysis (XRD). Further characterization of the samples was also carried out using ^{29}Si Magic Angle Spinning NMR (MAS NMR) spectrometer and Electron Paramagnetic Resonance (EPR) for iron catalysts as well as the copper catalyst to study the silicon and metal environments in the structure. The textural properties such as the specific surface area, pore volume and average pore diameter were measured using nitrogen gas adsorption-desorption analysis. The thermal stability of the samples was determined by utilizing thermogravimetry analysis coupled with Fourier Transform-Infrared spectrometer (TGA-FT-IR). The diffuse reflectance UV-Vis (DR UV-Vis) had been also obtained for the samples in order to study the coordination environment of the metal. The surface acidity of the samples was monitored by Fourier Transform-Infrared (FT-IR) spectroscopy of adsorbed pyridine.

The final part of this study is to test the catalytic activity of the as-synthesized catalysts and calcined catalyst towards Friedel-Crafts benzoylation of aromatics (*p*-xylene, anisole and toluene) with benzoyl chloride as the benzoylating agent. The products were analyzed by gas chromatography (GC) and the identification of products was carried out using gas chromatography with the mass spectrometry detector (GC-MS) and with the authentic pure samples.

1.6 Research objectives

The objectives of this research are listed as follows:

- To prepare RHA-xFe (x = 5, 10, 15 and 20 wt.%), RHA-10Cu and RHA-10Sn catalysts using rice husk ash as the silica source via the sol-gel method.
- To characterize these modified catalysts in detail by various physico-chemical and spectroscopic techniques such as XRD, FT-IR, N_2-sorption,

AAS, SEM-EDX, TEM, DR UV/Vis, solid state ^{29}Si MAS NMR, EPR, TGA-FTIR and FT-IR-pyridine adsorption.

- To study the catalytic activity of as-synthesized catalysts in the Friedel-Crafts benzoylation reaction using benzoyl chloride as benzoylating agent for *p*-xylene, anisole and toluene.
- To study the difference between heterogeneous, homogeneous and calcined catalysts.
- To study the effect of metal loadings, catalyst mass, molar ratio, reaction temperature, catalyst type, catalyst stability and catalyst reusability on the Friedel-Crafts benzoylation reaction.
- To study kinetics of Friedel-Crafts benzoylation reaction.

Experimental

2.1 Raw material and chemicals

The rice husk which was used as a silica source in this study was supplied by Leong Guan Sdn. Bhd, a local rice mill, situated in Seberang Perai Utara, Penang. The chemicals used were nitric Acid (HNO_3, Systerm®- ChemAR®, 65.0%), sodium hydroxide-pellets (NaOH, Systerm®- ChemAR®, 99.0%), iron (III) nitrate-nonahydrate ($Fe(NO_3)_3.9H_2O$, Systerm®- ChemPur®, > 98.0%), copper (II) nitrate ($Cu(NO_3)_2.3H_2O$, R&M Chemicals, 99.0%), tin (II) chloride (anhydrous) ($SnCl_2$, Sigma-Aldrich, 98.0%), anisole (Merck, ≥ 99.0% (GC)), *p*-xylene (Fluka, ≥ 98.0% (GC)), toluene (R&M Chemicals, 99.0% (GC)), decane (Acrõs- Organics, 99+%), benzoyl chloride (Fluka- Chemika, ≥ 98.0%), benzoic acid (Systerm®- AR, 99.0%), benzoic anhydride (Fluka, ≥ 95.0%), *o*-methylbenzophenone (Aldrich, 98.0% (GC)), *m*-methylbenzophenone (Aldrich, 99.0%), *p*-methylbenzophenone (Aldrich, 99.0% (GC)), *p*-methoxybenzophenone (Fluka, ≥ 98.0% (GC)). All these reagents were used directly without further purification.

2.2 Catalysts preparation

2.2.1 Treatment of rice husk

The rice husk (RH) was washed with copious amount of tap water to remove the adhering soil, dirt and contaminants such as tiny stones and other unwanted particles. During the washing process, only the RH that settled at the bottom was collected to ensure consistency. It was rinsed with distilled water three times and dried at room temperature for 48 h. About 100 g of this clean RH was stirred in 2 L of 1.0 M nitric acid at room temperature using an overhead stirrer (Model

RW20DZM.n, Kika Labortechnik) for 24 h to remove all metals originating from the soil during the lifetime of the rice plant. The acid treated RH was washed thoroughly with distilled water until the pH of the rinse became constant (pH meter, Model pH 510, Eutech Instruments). The wet RH was subsequently dried in an oven at 110 °C for 18 h and burned in a muffle furnace (Model AAF 11/7, Carbolite, UK) at 800 °C for 6 h for complete combustion. The white rice husk ash (RHA) thus obtained was further treated with 1.0 M HNO_3 for 24 h to reduce all metallic impurities to negligible levels. It was filtered and washed thoroughly with distilled water until a constant pH and dried at 110 °C overnight. The treated RHA was used as silica source for the preparation of the catalysts.

2.2.2 Extraction of silica as sodium silicate

About 5.0 g of the treated RHA was added to 250 mL of 1.0 M NaOH in a plastic container and stirred for 18 h at room temperature using a magnetic stirrer (Model nuova 7, Sybron/Thermolyne, USA) to extract the silica as sodium silicate. The solution was filtered to remove un-dissolved particles through Whatman No. 41 ash less filter paper to yield a clear solution of sodium silicate.

2.2.3 Preparation of silica

The extracted sodium silicate solution was titrated with 3.0 M HNO_3. The acid solution was added at a slow rate (1.0 mL min^{-1}) with constant stirring by controlling the pH of the solution. The precipitation of silica gel was started at pH 10. The titration was continued until pH 5. This suspension was kept in a covered plastic container for ageing (24 h). The silica gel formed was centrifuged (Model T 30, JANETZKI), washed with distilled water followed by acetone, filtered through

Whatman No. 41 ash less filter paper and dried at 110 °C for 18 h. The material was ground to powder and washed again with distilled water several times to improve the purity of silica by removing mineral impurities (Kalapathy *et al.*, 2000a; Kalapathy *et al.*, 2002), then filtered and dried at 110 °C for 18 h. The silica obtained was labeled as RHA-SiO_2.

2.2.4 Preparation of iron-rice husk silica

Iron incorporated rice husk silica catalysts were prepared by the same procedure as for silica except, mass of 1.81, 3.62, 5.43 and 7.23 g of $Fe(NO_3)_3.9H_2O$ salt were separately dissolved in 3.0 M HNO_3 and these solutions were titrated with the sodium silicate solution (~ 1.0 mL min^{-1}) with continuous stirring until pH 5 to prepare 5, 10, 15 and 20 wt.% iron loaded catalyst respectively. The resulting gel was aged for 24 h at room temperature. The gel formed was separated by centrifuge, washed with distilled water followed by acetone and dried at 110 °C for 18 h. The samples were ground to powder and washed again with distilled water, filtered and dried at 110 °C for 18 h. The catalysts obtained were labeled as RHA-xFe (x = 5, 10, 15 and 20 wt.%) and ~ 5 g of the powder was obtained for each sample. A portion of the RHA-10Fe was calcined at 500 °C for 5 h and denoted as RHA-10Fe(Cal).

2.2.5 Preparation of copper-rice husk silica

To prepare 10 wt.% copper incorporated rice husk silica, 1.90 g of $Cu(NO_3)_2.3H_2O$ salt was separately dissolved in 3.0 M HNO_3 and this solution was used to titrate the sodium silicate solution until pH 5. The copper incorporated silica gel was recovered and processed as previously mentioned for the preparation of iron-rice